International Journal of Science and Engineering Applications
Volume 10-Issue 04, 29 - 33, 2021, ISSN:- 2319 - 7560

The Effects of Pine Tree Sawdust on the Volume Compressibility of Expansive Soils

Ekrem Kalkan
Department of Civil Engineering
Engineering Faculty
Ataturk University
Erzurum, Turkey

Necmi Yarbaşı
Department of Civil Engineering
Engineering Faculty
Ataturk University
Erzurum, Turkey

Abstract: Expansive soils are very important natural geological materials used in the geotechnical applications in the worldwide. After compacting, they are used as hydraulic barriers in earth structures, such as core of earth fill dams, landfill liners, and etc. However, these soils have some defects from technical points of view. To remove the defects, one of the soil improvement methods is mixing of these soils with granular materials. In this study, pine tree sawdust was used as granular additive material to stabilize the expansive soils. The effects of pine saw dust on the volume compressibility of expansive soils were investigated by using experimental studies under laboratory conditions. The test results showed that the pine saw dust positively affected the geotechnical properties in term of volume compressibility manner. As a consequently, the geotechnical properties of the expansive soil when blended with pine tree sawdust indicates that the pine tree sawdust is a good modification material for this problematic soil.

Keywords: Expansive soil, waste material, pine tree sawdust, soil stabilization, volume compressibility

1. INTRODUCTION

The soil is one of the oldest and perhaps most complex geological materials that humanity has been working on. Various problems have begun to be encountered by using the expansive soil as foundation or material. The expansive soil changes in volume in relation to changes in water content. This occurs as swelling upon wetting, and shrinkage upon drying. These soils have poor volume stability in the presence of water (Jones and Jefferson, 2012; Li et al., 2014; Khanduri, 2020). These soils have a problem worldwide undergoing considerable volume changes such as swelling on absorbing water and shrinking on evaporation.

Moreover, moisture fluctuations of them cause distinct changes in soil strength (Fredlund and Rahardjo, 1993; Sheng et al., 2008; Phanikumar, 2009; Lin, and Cerato, 2012; Poonia et al., 2019). Such soils should generally be avoided for the purpose of construction. Because, the structural damages of constructures built on expansive soils is well documented in literature (Petry and Little, 2002; Fall and Sarr, 2007; Kalkan and Bayraktutan, 2008; Ozer et al., 2011; Jones and Jefferson, 2012; Tiwari et al., 2012; Kalkan et al., 2019; James, 2020; Kalkan et al., 2020; Yarbaşı and Kalkan, 2020a). Also, the damage to lightly loaded structures founded on expansive soils has been widely reported (Cameron et al., 1987; Walsh and Cameron, 1997; Fityus et al., 2004; Delaney et al., 2005; Miao et al., 2012; Li et al., 2014; Kalkan et al., 2015).

The soil is one of the most important and primary media for any construction work. The strength and durability of any structure depends on the strength properties of soil (Nath et al., 2017). Soil stabilization is defined as a technique to improve the engineering characteristics in order to improve the parameters such as shear strength, compressibility, density, hydraulic conductivity. The techniques of soil stabilization can be classified into a number of categories such as vibration, surcharge load, structural reinforcement improvement by structural fill, admixtures, and grouting and other methods. There are many techniques that can be used for different purposes by enhancing some aspects of soil behavior and improve the strength and properties of soil (Edil, 2003; Kazemain and Barghchi, 2012).

In some geotechnical engineering projects, such as core of earth fill dams, landfill liners, and etc, to achieve lower values of hydraulic conductivity it requires to compact clayey soils at wet of optimum water content. Shear strength of clayey soils in general is relatively low and when they subject to seasonal drying, loss of water occurs due to desiccation that alters their properties, including reduction in soil plasticity, possible cracking, and increasing of hydraulic conductivity (Soltani-Jigheh and Jafari, 2012).

Expansive soils pose the problem of swelling on absorption of water during monsoon and shrinkage on evaporation of water in summer (Chen, 1988, McKeen 1988; Nelson and Miller, 1992; Kenneth, 1993). As a result of the swell-shrink behavior of expansive soils, lightly loaded structures such as foundations, pavements, canal beds, and linings and residential buildings founded in them are severely damaged (Chen, 1988).

The several researchers have investigated the effect of granular material on the mechanical properties of mixed clayey soils (Holtz and Willard, 1956; Nakase et al., 1978; Shakoor and Cook, 1990; Shelley and Daniel, 1993; Howell et al., 1997). Vallejo and Mawby (2000) carried out direct shear tests on mixtures of Ottawa sand-kaolin clay and found that shear strength of the mixtures depends upon their sand contents (Soltani-Jigheh and Jafari, 2012).

Several soil stabilization methods are available for stabilization of expansive clayey soils. These methods include the use of chemical additives, rewetting, soil replacement, compaction control, moisture control, surcharge loading, and thermal methods (Chen, 1988; Nelson and Miller, 1992; Yong and Ouhadi, 2007). Many investigators have studied natural, fabricated, and by-product materials and their use as additives for the stabilization of clayey soils (Kalkan, 2020; Kalkan and Yarbaşı, 2020; Kalkan et al., 2020; Yarbaşı and Kalkan, 2020a; Yarbaşı and Kalkan, 2020b; Yarbaşı and Kalkan, 2020c).

Soil stabilization is one of the most widely followed techniques to control the swelling behavior of expansive soils in lightly loaded structures (Selvakumar and Soundara, 2019). The stabilization techniques to control the swelling characteristics in expansive soils can be grouped into mechanical, chemical and polymer as well as unconventional stabilizer methods (Petry and Little, 2002; Ikizler et al., 2009; Estabragh et al., 2014; Kalkan et al., 2019; Kalkan, 2020; Yarbaşı and Kalkan, 2020a). In the chemical stabilization, some additives such as lime, cement, fly ash, silica fume etc., are added, which physically interacts with the soil and change the index properties (Chen, 1988; Çokça, 2001; Kalkan and Akbulut, 2004; Kalkan, 2009; Kalkan, 2011; Jamsawang et al., 2017; Chittoori et al., 2018; Kalkan et al., 2019). In recent times, the use of polymer-based product such as geosynthetics in expansive soil stabilization (Al-Omari and Hamodi, 1991; Sharma and Phanikumar, 2005; Viswanadham et al., 2009; Buzzi et al., 2010) is widely practiced due to their desirable properties and durability (Jewell, 1991; Koerner, 1999; Selvakumar and Soundara, 2019).

In this study, the pine tree sawdust was used as alternative low-cost stabilizer material. The main objectives of this research are to investigate the utilizable of pine tree sawdust as additive material for stabilization of expansive soils in geotechnical applications in term of volume compressibility manner. The stabilized expansive soils were subjected the consolidation tests and the results obtained were compared with that of natural expansive soils

2. MATERİLA and METHODS

2.1. Materials

The expansive soil material was supplied from the clayey soil deposits of Oltu-Narman sedimentary basin, Erzurum, NE Turkey. The expansive soil samples were taken 0,75 m deep. According to the United Soil Classification System, expansive soil are inorganic clays of high plasticity (CH). These soils have high expansion potential as a result of over consolidation, high-very high plasticity and montmorillonite content (Kalkan, 2003; Kalkan and Bayraktutan, 2008). The grain-size distribution of expansive soil was given in Figure 1.

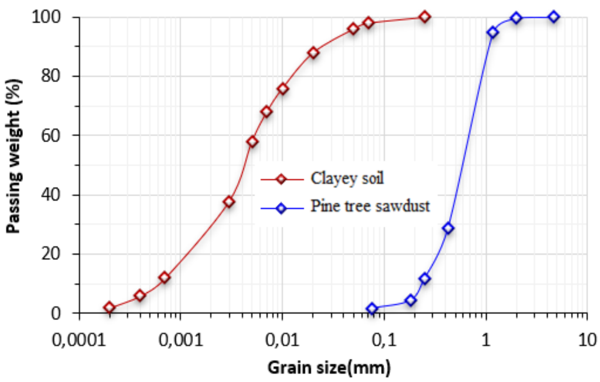

Figure 1. Grain size distribution of expansive soil and pine tree sawdust

Wood cutting factories, generates a by-product known as sawdust. The pine tree sawdust waste material was obtained from the carpenters in the industrial zone of Oltu (Erzurum), NE Turkey. The pine tree sawdust is an organic waste resulting from the mechanical milling or processing of timber (wood) into various standard shapes and useable sizes. Consisting of soil-like particulate materials that are lighter than soil, sawdust inexpensive and environmentally safe (Rao et al., 2012; Oyedepo et al., 2014). The grain-size distribution of pine tree sawdust was illustrated in the Figure 1.

2.2. Methods

2.2.1. Preparation of samples

Before preparation of samples, the expansive soil and pine tree sawdust materials were mixed at the different contents of them. Under dry condition, expansive soil and pine tree sawdust materials were mixed to prepare mixtures of expansive soil-pine tree sawdust. The amounts of pine tree sawdust were selected to be 0,5%, 1% and 1,5 % of the total dry weight of the mixtures (Table 1). The dry mixtures were mixed with the required amount of water recognized to give the optimum water content. All mixing was done manually and proper care was taken to prepare homogeneous mixtures at each stage.

Table 1. The expansive soil and pine tree rates of mixtures

Samples	Expansive soil (%)	Pine tree sawdust (%)	Total (%)
MIX0	100	-	100
MIX1	99,5	0,5	100
MIX2	99,0	1,0	100
MIX3	98,5	1,5	100

2.2.2. Standard odometer test

The compressibility behaviors of expansive soil and expansive soil-pine tree sawdust mixtures were assessed from standard odometer tests. The standard oedometer test is a classical laboratory test that allows characterizing the soil stress-strain behavior during one-dimensional compression or swelling. The samples compacted at their optimum moisture content in a standard proctor mold and then extruded using a cutting ring were subjected to one dimensional consolidation tests in accordance with ASTM D 2435.

3. Results and Discussion

3.1. Effects of pine tree sawdust on the coefficient of volume compressibility

The effects of pine tree sawdust on the coefficient of volume compressibility (mv) of pine tree sawdust-modified expansive soil were illustrated in Figure 2. The mv of pine tree sawdust-modified expansive soil samples significantly increased with addition of more pine tree sawdust content up to 0,5%, 1% and 1,5%. Contrary to this situation, the consolidation coefficient (cv) increases (Figure 3). These mv and cv value were varied at the same consolidation pressure and its might be due to content of clay mineral in the pine tree sawdust-modified expansive soil (Shirazi et al., 2010). The decrease in the void ratio and compressibility of pine tree sawdust-modified expansive soil samples was attributed to the addition of low plastic material and the interaction between clayey minerals and pine tree sawdust particles (Kalkan and Akbulut, 2004). A large number of researchers studied the effect of mineral composition on the compressibility and swelling behavior of expansive soil (Mesri and Olson, 1971; Mitchell, 1993; Di Maio et al., 2004).

3.2. Image Study

Figures 4a and 4b show SEM micrographs of natural expansive soil and 0,5% pine tree sawdust-modified expansive soil samples, respectively. It is seen from the images that the addition of pine tree sawdust to the expansive soil caused the structural change pine tree sawdust-modified expansive soil samples. Silt and clay grains of expansive soil showed angular or subangular shapes (Figure 4a).

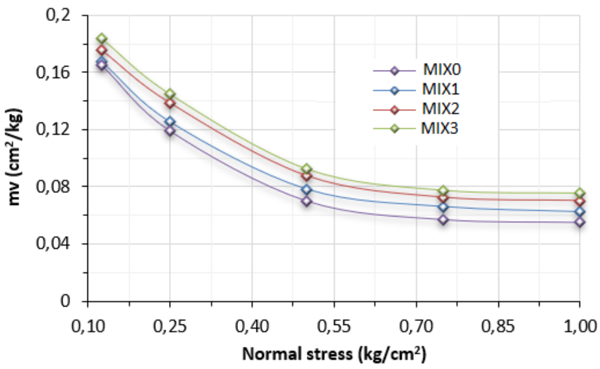

Figure 2. The change in the volumetric compression coefficients of samples

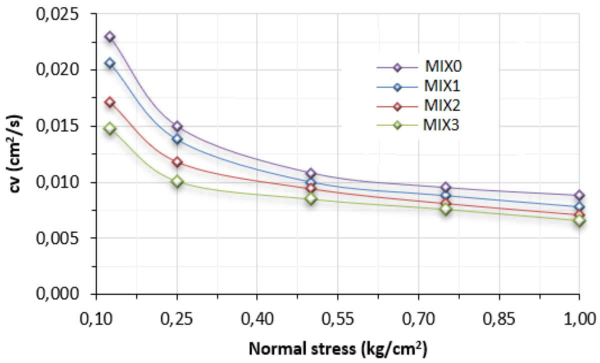

Figure 3. The change in consolidation coefficients of samples

In the 0,5% pine tree sawdust stabilized samples (MIX1), all grains were covered by relatively thick pine tree sawdust material, which formed cementing medium. This textural event caused a significant improvement in the geotechnical properties. A detailed examination of each micrograph reveals that most of the flocculation products are deposited on the surfaces of the soil grains or at the contact points (Fig. 4b). The bonding of particles into larger aggregates such that the soil behaved as a fine-grained, strongly bonded particulate material (Okyay and Dias, 2010).

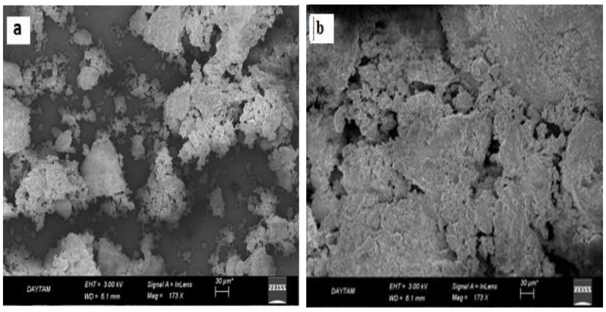

Figure 4. The SEM images of MIX0 and MIX1

4. CONCLUSIONS

In this study, the effects of pine tree sawdust on the compressibility behavior of expansive soils. According to the test results, additive of pine tree sawdust improved the compressibility behavior of expansive soil samples. As a result, the pine tree sawdust can be used as an additive material for the stabilization of the expansive soils in the geotechnical applications in term of the compressibility behavior of expansive soils.

4. REFERENCES

[1] Al-Omari, R.R., Hamodi, F.J., 1991. Swelling resistant geogrid-a new approach for the treatment of expansive soils. Geotextiles and Geomembranes 10, 295-317.
[2] Buzzi, O., Fityus, S., Sloan, S.W., 2010. Use of expanding polyurethane resin to remediate expansive soil foundations. Canadian Geotechnical Journal 47 (6), 623-634.
[3] Cameron, D.A., Walsh, P.F., Richards, B.G., 1987. Australian approach to the problem of expansive soils. In: Proccedings of 9th Regional Conference for Africa on Soil Mechanics and Foundation Engineering, Lagos, p. 977-989.
[4] Chen, F.H., 1988. Foundations on Expansive Soils. Elsevier Science Publishing Company, Amsterdam.
[5] Chittoori, B.C., Mishra, D., Islam, K.M., 2018. Forensic investigations into recurrent pavement heave from underlying expansive soil deposits. Transportation Research Record Journal of the Transportation Research Board, 0361198118758625.
[6] Çokça, E., 2001. Use of class C fly ashes for the stabilization of an expansive soil. Journal of Geotechnical and Geoenvironmental Engineering 127 (7), 568-573.
[7] Delaney, M.G., Li, J., Fityus, S.G., 2005. Field monitoring of expansive soil behavior in the Newcastle-hunter region. Australian Geomechanics Journal, 6 (2), 3-14.
[8] Di Maio, C., Santoli, L., Schiavone, P., 2004. Volume change behaviour of clays: the influence of mineral composition, pore fluid composition and stress state. Mechanics of Materials 36, 435-451.
[9] Edil, T.B., 2003. Recent advances in geotechnical characterization and construction over peat and organic soils" Proceeding's 2nd International Conference on Advances in Soft Soil Engineering and Technology. (Eds). Huat et al. Malaysia: Putrajaya, pp. 3-25.
[10] Estabragh, A.R., Rafatjo, H., Javadi, A.A., 2014. Treatment of an expansive soil by mechanical and chemical techniques. Geosynthetics International 21 (3), 233-243.
[11] Fall, M., Sarr, A.M., 2007. Geotechnical characterization of expansive soils and their implications in ground movements in Dakar. Bulletin of Engineering Geology and the Environment 66 (3), 279-288.
[12] Fityus, S.G., Smith, D.W., Allman, M.A., 2004. An expansive soil test site near Newcastle. ASCE Journal of Geotechnical and Geoenvironmental Engineering 130 (7), 686-695.
[13] Fredlund, D.G., Rahardjo, H., 1993. Soil mechanics for unsaturated soils. United States of America: John Wiley & Sons.
[14] Holtz, W.G., Willard, M., 1956. Triaxial shear characteristics of clayey gravel soils. Soil Mechanics and Foundation Engineering 82, 143-149.

[15] Howell, J.L., Shackelford, C.D., Amer, N.H., Stern, R.T., 1997. Compaction of sand processed clay soil mixtures. Geotechnical Testing Journal 20 (4), 443-458.
[16] Ikizler, S.B., Aytekin, M., Vekli, M., 2009. Reductions in swelling pressure of expansive soil stabilized using EPS geofoam and sand. Geosynthetics International 16 (3), 216-221.
[17] James, J., 2020. Sugarcane press mud modification of expansive soil stabilized at optimum lime content: Strength, mineralogy and microstructural investigation. Journal of Rock Mechanics and Geotechnical Engineering 12, 395-402.
[18] Jamsawang, P., Nuansrithong, N., Voottipruex, P., Songpiriyakij, S., Jongpradist, P., 2017. Laboratory investigations on the swelling behavior of composite expansive clays stabilized with shallow and deep clay-cement mixing methods. Applied Clay Sciences 148, 83-94.
[19] Jewell, R.A., 1991. Application of revised design charts for steep reinforced slopes. Geotextile and Geomembranes 10 (3), 203-233.
[20] Kalkan, E., 2003. The improvement of geotechnical properties of Oltu (Erzurum) clayey deposits for using them as barriers. PhD Thesis (in Turkish), Ataturk University, Graduate School of Natural and Applied Science, Erzurum, Turkey.
[21] Kalkan, E., 2009. Influence of silica fume on the desiccation cracks of compacted clayey soils. Applied Clay Science 43, 296-302.
[22] Kalkan, E., 2011. Impact of wetting-drying cycles on swelling behavior of clayey soils modified by silica fume. Applied Clay Science 52, 345-352.
[23] Kalkan, E., 2020. A Review on the Microbial Induced Carbonate Precipitation (MICP) for Soil Stabilization. International Journal of Earth Sciences Knowledge and Applications 2 (1), 38-47.
[24] Kalkan, E., Akbulut, S., 2004. The positive effects of silica fume on the permeability, swelling pressure and compressive strength of natural clay liners. Engineering Geology 73, 145–156.
[25] Kalkan, E., Bayraktutan, M.S., 2008. Geotechnical evaluation of Turkish clay deposits: a case study in Northern Turkey. Environmental Geology 55, 937-950.
[26] Kalkan, E., Nadaroglu, H., Celebi, N., Celik, H., Tasgin, E., 2015. Experimental Study to Remediate Acid Fuchsin Dye Using Laccase-Modified Zeolite from Aqueous Solutions. Polish Journal of Environmental Studies 24 (1), 115-124.
[27] Kalkan, E., Yarbaşı, N., 2020. The effect of waste material mixtures on the mechanical properties of clayey soils. International Journal of Latest Technology in Engineering, Management and Applied Science (IJLTEMAS) 11 (10), 48-52.
[28] Kalkan, E., Yarbasi, N., Bilici, O., 2019. Strength performance of stabilized clayey soils with quartzite material. International Journal of Earth Sciences Knowledge and Applications 1 (1)1-5.
[29] Kalkan, E., Yarbasi, N., Bilici, O., 2020. The Effects of Quartzite on the Swelling Behaviors of Compacted Clayey Soils. International Journal of Earth Sciences Knowledge and Applications 2 (2), 92-101.
[30] Kazemain, S., Barghchi, M., 2012. Review of soft soils stabilization by grouting and injection methods with different chemical binders. Scientific Research and Essays 7 (24), 2104-2111.
[31] Kenneth, D., 1993. Evaluation of In-Place Wetting Using Soil Suction Measurements. Journal of Geotechnical Engineering, ASCE, 119 (5), 862-873.
[32] Khanduri, S., 2020. Cloudbursts Over Indian Sub-continent of Uttarakhand Himalaya: A Traditional Habitation Input from Bansoli, District-Chamoli, India. International Journal of Earth Sciences Knowledge and Applications 2 (2), 48-63.
[33] Koerner, R.M., 1999. Designing with Geosynthetics. Prentice-Hall, Upper Saddle River, N.J.
[34] Li, J., Cameron, D.A., Ren, G., 2014. Case study and back analysis of a residential building damaged by expansive soils. Computers and Geotechnics 56, 89-99.
[35] Lin, B., Cerato, A., 2012. Investigation on soil-water characteristic curves of untreated and stabilized highly clayey expansive soils. Geotechnical and Geological Engineering 30 (4), 803-812.
[36] McKeen, R.G., 1988. Soil Characterization Using Suction Measurements", Proceedings, 25th Paving and Transportation Conference, University of New Mexico, Albuquerque, N.M.
[37] Mesri, G., Olson, R.E., 1971. Consolidation characteristics of montmorillonite, Geotechnique 21 (4), 341-352. 1971.
[38] Miao, L., Wang, F., Cui, Y., Shi, S.B., 2012. Hydraulic characteristics, strength of cyclic wetting-drying and constitutive model of expansive soils. In: Proceedings of 4th International Conference on Problematic Soils, Wuhan, China, p. 303-322.
[39] Mitchell, J.K. 1993. Fundamentals of soil behavior. 2nd Ed., 1993. Wiley, New York.
[40] Nath, B.D., Molla, M.K.A., Sarkar, G., 2017. Study on Strength Behavior of Organic Soil Stabilized with Fly Ash. International Scholarly Research Notices 2017, 5786541.
[41] Nakase, A., Nakanodo, H., Kusakabe, O., 1978. Influence of soil type on pore pressure response to cyclic loading. In Proceeding of 5th Japan Earthquake Engineering Symposium, 593-600.
[42] Nelson, D.J., Miller, J.D., 1992. Expansive Soils: Problems and Practice in Foundation and Pavement Engineering", Wiley, New York.
[43] Okyay, U.S., Dias, D., 2010. Use of lime and cement treated soils as pile supported load transfer platform. Engineering Geology 114, 34-44.
[44] Oyedepo, O.J, Oluwajana, S.D., Akande, S.P., 2014. Investigation of Properties of Concrete Using Sawdust as Partial Replacement for Sand. Civil and Environmental Research 6 (2), 35-42.
[45] Ozer, M., Ulusay, R., Isik, N.S., 2011. Evaluation of damage to light structures erected on a fill material rich in expansive soil. Bulletin of Engineering Geology and the Environment 71 (7), 1-33.
[46] Petry, T.M., Little, D.N., 2002. Review of stabilization of clays and expansive soils in pavements and lightly loaded structures e history, practice, and future. Journal of Materials in Civil Engineering 14(6), 447-460.
[47] Phanikumar, B.R., 2009. Effect of lime and fly ash on swell, consolidation and shear strength characteristics of expansive clays: a comparative study. Journal Geomechanics and Geoengineering 4 (2), 175-181.
[48] Phanikumar, B.R., Amshumalini, C., Karthika, R., 2009. Volume Change Behavıour of Expansıve Clay-Sand Blends. IGC 2009, Guntur, India.
[49] Poonia, J., Giustozzia, F., Roberta, D., Setungea, S., O'Donnellb, B., 2019. Durability of enzyme stabilized expansive soil in road pavements subjected to moisture degradation. Transportation Geotechnics 21, 100225.
[50] Rao, D.K., Anusha, M., Pranav, P.R.T., Venkatesh, G.,

2012. A laboratory study on the stabilization of marine clay using saw dust and lime. International Journal of Engineering Science and Advanced Technology 2 (4), 851-862.

[51] Selvakumar, S., Soundara, B., 2019. Swelling behavior of expansive soils with recycled geofoam granules column inclusion. Geotextiles and Geomembranes 47, 1-11.

[52] Shakoor, A., Cook, B.D., 1990. The effect of stone content, size and shape on engineering properties of compacted silty clay. Bulletin of the Association of Engineering Geologists 27, 245-253.

[53] Sharma, R.S., Phanikumar, B.R., 2005. Laboratory study of heave behavior of expansive clay reinforced with geopiles. Journal of Geotechnical and Geoenvironmental Engineering 131 (4), 512-520.

[54] Shelly, T.L., Daniel, D.E., 1993. Effect of gravel on hydraulic conductivity of compacted soil liners. Journal of Geotechnical Engineering 119, 54-68.

[55] Sheng, D., Gens, A., Fredlund, D.G., Sloan, S.W., 2008. Unsaturated soils: From constitutive modelling to numerical algorithms. Computer and Geotechnics 35 (6), 810-824.

[56] Shirazi, S.M., Kazama, H., Salman, F.A., Othman, F., Akib, S., 2010. Permeability and swelling characteristics of bentonite. International Journal of the Physical Sciences 5 (11), 1647-1659.

[57] Soltani-Jigheh, H., Jafari, K., 2012. Volume Change and Shear Behavıor of Compacted Claysand/Gravel Mıxtures. International Journal of Engineering and Applied Sciences 4 (1), 52-66.

[58] Vallejo, L.E., Mawby, R., 2000. Void ratio Influence on the shear strength of granular material clay mixtures. Engineering Geology 58, 125-136.

[59] Viswanadham, B.V.S., Viswanadham, B.R., Mukherjee, R., 2009. Swelling behavior of a geofiber-reinforced expansive soil. Geotextiles and Geomembranes 27 (1), 73-76.

[60] Walsh, P.F, Cameron DA., 1997. The design of residential slabs and footings. Standards Australia, SAA HB28-1997.

[61] Yarbaşı, N., Kalkan, E., 2020a. Stabilization of Clayey Soils by Using the Organic Waste-Material. International Journal of Science and Engineering Applications 9 (11), 129-132.

[62] Yarbaşı, N., Kalkan E., 2020b. The Mechanical Performance of Clayey Soils Reinforced with Waste PET Fibers. International Journal of Earth Sciences Knowledge and Applications 2 (1) 19-26.

[63] Yarbaşı, N., Kalkan, E., 2020c. Investigation of Wet-Dry Cycle Effect on Swelling Behavior of Stabilized Expansive Soils. International Journal of Science and Engineering Applications 9 (12), 153-157.

[64] Yarbaşı, N., Kalkan, E., 2020d. Freeze-Thaw Resistance of Fine-Grained Soils Stabilized with Waste Material Mixtures. International Journal of Science and Engineering Applications 9 (12), 158-163.

[65] Yong, R.N., Ouhadi, V.R., 2007. Experimental study on instability of bases on natural and lime/cement-stabilized clayey soils. Applied Clay Science 35, 238-249.

Design, Analysis and Simulation of a Single Stage Rocket (Launch Vehicle) Using RockSim

Benneth Ifenna Okoli
National Space Research and Development Agency
Abuja, Nigeria.
Centre for Space Transport and Propulsion, Epe, Lagos.

Olusegun Samuel Sholiyi
National Space Research and Development Agency
Abuja, Nigeria.
Centre for Space Transport and Propulsion, Epe, Lagos.

Rasheed Olalekun Durojaye
National Space Research and Development Agency
Abuja, Nigeria.
Centre for Space Transport and Propulsion, Epe, Lagos.

This project describes the design, analysis, assembly and simulation of a single stage model rocket systems, one designed with traditional subsystems for structural, avionics, combustion chamber and recovery integrated to give a desired altitude. The analysis was based on using Rocksim 9.6 to model the different parts that made up a rocket. Aluminium was used for designing the nose cone, the fuselage and the fin set. The combustion chamber, clamps, and nozzle were designed by making use of steel. Because of the high temperature and pressure being generated from the combustion of propellant, steel was suggested. The main and drogue parachutes were designed using tubular Kevlar. And the bulk-head was designed using Basswood. For the recovering of the rocket after launch, main and drogue parachutes were incorporated into the fuselages.

Keywords: Rocket; aluminium; combustion chamber; nozzle; bulk-head; fuselage; parachute.

1. INTRODUCTION

Rockets are devices that contain all the elements necessary for propulsion within themselves. They are most useful for space travel and when high thrust rapid acceleration is required. Applications include boosting payloads to low-earth orbit, missiles, satellite station-keeping and orbit transfers, and interplanetary missions. Rockets are typified by the high velocity of the gas that is accelerated through a supersonic nozzle to generate thrust. They can be further classified according to the propellant state, the thrust level, and the type of engine cycle that is used [3]. A rocket design can be as simple as a cardboard tube filled with black powder, but to make an efficient, accurate rocket or missile involves design, simulation and construction of the different parts that made up a rocket. A rocket is made up of some major systems:

- The Structural System
- The Payload System
- The Control and Guidance System, and,
- The Propulsion System, etc. [1]

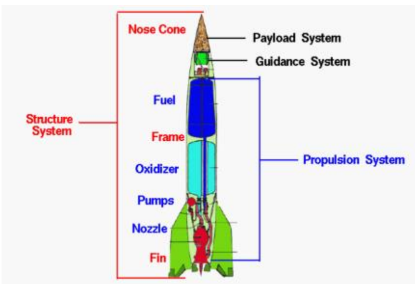

Figure 1: Major rocket systems [2].

The structural system, or frame, is similar to the fuselage of an airplane which is made up of the nose cone, fuselage (body tube) and the fins. The frame is made from very strong but light weight materials, like titanium or aluminium, and usually employs long "stringers" which run from the top to the bottom which are connected to "hoops" which run around the circumference. The nose cone is the tip of the rocket. It could be made of different shapes, conical, ogive, etc. This allows for minimum aerodynamic drag or resistance. The fuselage or frame of the rocket is usually in a vessel form. It serves as a support for the rocket. It houses the recovery system and the combustion chamber. The fins are also attached to the fuselage. Fins are attached to some rockets at the bottom of the frame to provide stability during the flight [2]. The payload system of a rocket depends on the rocket's mission. The earliest payloads on rockets were fireworks for celebrating holidays. Following World War II, many countries developed guided ballistic missiles armed with nuclear warheads for payloads. The same rockets were modified to launch satellites with a wide range of missions; communications, weather monitoring, spying, planetary exploration, and observatories, like the Hubble Space Telescope. Special rockets were developed to launch people into earth orbit and onto the surface of the Moon [2]. The guidance system of a rocket may include very sophisticated sensors, on-board computers, radars, and communication equipment to maneuver the rocket in flight. Many different methods have been developed to control rockets in flight. The V2 guidance system included small vanes in the exhaust of the nozzle to deflect the thrust from the engine. Modern rockets typically rotate the nozzle to maneuver the rocket. The guidance system must also provide some level of stability so that the rocket does not tumble in flight [2]. There are two main classes of propulsion systems, liquid rocket engines and solid rocket engines. The V2 used a liquid rocket engine consisting of fuel and oxidizer (propellant) tanks, pumps, a combustion chamber with nozzle, and the associated plumbing. The Space Shuttle, Delta II, and Titan III all use solid rocket strap-ons [2]. The various rocket parts described above have been grouped by function into structure, payload, guidance, and propulsion systems. There are other possible groupings. For the purpose of weight determination and flight performance, engineers often group the payload, structure, propulsion structure (nozzle, pumps, tanks, etc.), and guidance into a single empty weight parameter. The remaining propellant weight then becomes the only factor that changes with time when determining rocket performance [2].

1.1 Material selection criteria

In rocket designs, material selection for the components or structure of a launch vehicle is of paramount importance. In the selection of materials for the rocket, it is desirable to use a material that has high-to-weight ratio, good mechanical properties and ease of fabrication. Choice of material considerations:

- Strength (Tensile, Compressive, etc).
- Availability of material
- Affordability/cost effectiveness
- Ease of fabrication
- Corrosion resistance
- Fracture toughness
- Thermal expansivity and conductivity
- Melting point of material [1].

2. DESIGN PARAMETERS FOR A SINGLE STAGE ROCKET [1]

2.1 Rocket structure dimensions:

2.1.1 Nose cone

We chose Aluminium because of its properties and heritage.

Thickness of Aluminum sheet used: 0.1 cm

Diameter of rocket = 30.2 cm

Total length of rocket = 384 cm

Fineness Ratio i.e. ratio of height to diameter of the rocket: L/D = 12.7

Front diameter of nose cone = 2 cm

Rear diameter of nose cone = 29.8 cm

Length of nose cone = 45 cm

2.1.2 Nose cone extension

We chose Alumnium because of its properties and heritage.

Thickness of Aluminum sheet used: 0.1 cm

Outer diameter = 29.8 cm

Inner diameter = 29.6 cm

Length = 20 cm

Location: 45 cm

2.1.3 Payload

We chose steel because of its properties and heritage.

Outer diameter = 6 cm

Inner diameter = 5.5 cm

Length = 20 cm

Location: 7.72 cm

2.1.4 Body tube 1

We chose Aluminium because of its properties and heritage.

Thickness of Aluminum sheet used: 0.1 cm

Outer diameter = 30.2 cm

Inner diameter = 30 cm

Length = 100 cm

2.1.5 Bulkhead (ring component)

We chose Basswood because of its properties and heritage.

Thickness: 1 cm

Outer diameter = 30 cm

Inner diameter = 0 cm

2.1.6 Electronics (Avionics) Bay

We chose Aluminium because of its properties and heritage.

Thickness: 0.1 cm

Outer diameter = 29.8 cm

Inner diameter = 29.6 cm

Location = 0.0

2.1.7 Electronics (Avionics) Bay stirp

We chose Aluminium because of its properties and heritage.

Thickness: 0.1 cm

Outer diameter = 30.2 cm

Inner diameter = 30 cm

2.1.8 Main Parachute

Material = ¼ in. tubular Kevlar

Thickness = 0.2 cm

Shape = round

Chute count = 1

Spill hole diameter = 18.8 cm

Drag coefficient = 0.75

Location = 23.10 cm

Shroud line material = ¼ in. tubular Kevlar

Shroud line length = 682 cm

Descent rate = 12.5678 m/s

Calculated descent rate mass = 70.9814428 kg

2.1.9 Body tube 2

We chose Alumnium because of its properties and heritage.

Thickness of Aluminum sheet used: 0.1 cm

Outer diameter = 30.2 cm

Inner diameter = 30 cm

Length = 180 cm

2.1.10 Fin sets

Fin count and shape = 4

Root chord length = 50 cm

Tip chord length = 25 cm

Sweep length = 24.162 cm

Sweep angle = 32.659 degrees

Semi span = 37.5 cm

Location = 130 cm

Thickness = 0.33 cm

Cross section = square

2.1.11 Combustion chamber

We chose steel because of its properties and heritage.

Outer diameter = 27 cm

Inner diameter = 26.079 cm

Location = 70 cm

2.1.12 Clamp 1

We chose steel because of its properties and heritage.

Outer diameter = 28.14 cm

Inner diameter = 27 cm

Location = 106 cm

2.1.13 Clamp 2

Outer diameter = 28.14 cm

Inner diameter = 27 cm

Location = 0.0 cm

2.1.14 Clamp 3

Outer diameter = 28.14 cm

Inner diameter = 27 cm

Location = 59.82 cm

2.1.15 Drogue Parachute

Shape = round

Outer diameter = 250 cm

Material = ¼ in. tubular Kevlar

Thickness = 0.33 cm

Spill hole diameter = 0.0 cm

Drag coefficient = 0.75

Location = 23.10 cm

Shroud line material = ¼ in. tubular Kevlar

Shroud line length = 455 cm

Shroud line count = 8

Descent rate = 17.5005 m/s

Calculated descent rate mass = 70.9814428 kg

2.1.16 Nozzle convergent

We chose steel because of its properties and heritage.

Thickness = 0.5 cm

Front diameter = 27 cm

Rear diameter = 8 cm

Length = 10 cm

2.1.17 Nozzle throat

Thickness = 0.5 cm

Outer diameter = 27 cm

Inner diameter = 8 cm

Length = 4 cm

2.1.18 Nozzle Divergent

Thickness = 0.5 cm

Front diameter = 8.2 cm

Rear diameter = 13 cm

Length = 15 cm

3. RESULTS AND DISCUSSIONS

Figure 2 below shows the Rocksim window for the design of the different parts that made up a single rocket as specified above, from the input parameters.

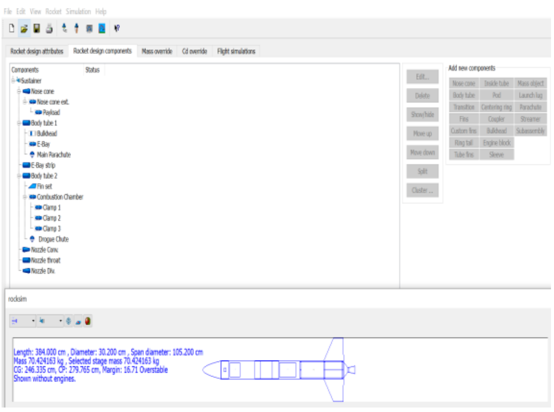

Figure 2: Rocksim window showing the different components of the rocket [4].

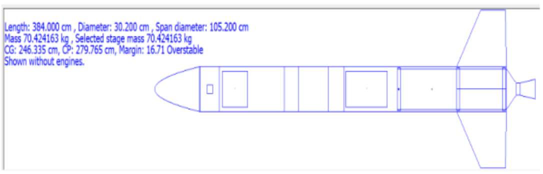

Figure 3: Exploded view of the rocket [4].

Figure 3 shows the designed rocket having a length of 384 cm, outer dimeter of 30.2 cm, and span diameter of 15.2 cm.

Figure 4 shows the designed rocket when the engine is loaded. The beauty of this propellant is the fact that it is an indigenous fuel designed, characterized, and produced at Centre for Space Transport and Propulsion, Epe, Lagos (CSTP) which is one of the Activities Centres of National Space Research and Development Agency, Abuja, Nigeria. As can be seen from Figure 4, the rocket has centres of gravity and pressure to be 275.635cm and 279.765 cm respectively, an indication that the rocket is stable. Also, the rocket has a positive margin of 2.06; which is a very aspect for the rocket to be stable during flight [4].

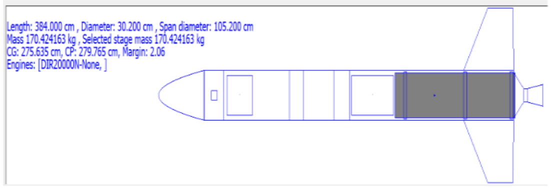

Figure 4: Loaded rocket engine [4].

The fuel is a solid propellant which has been tested and validated by team of scientists and engineers at CSTP. The advantages of having this engine added into the default software setting are that the propellant characterization, composition, and performance has been verified and validated through several static tests, unlike other engines in the default software which are like black-boxes and also, they are not readily available for the end users [5].

The 2-D profile of the rocket with engine at lift – off can be seen in Figure 5.

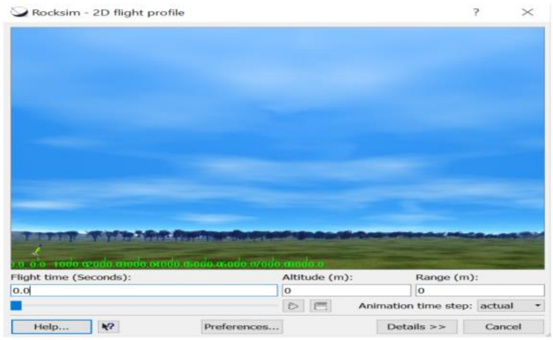

Figure 5: 2-D flight profile [4].

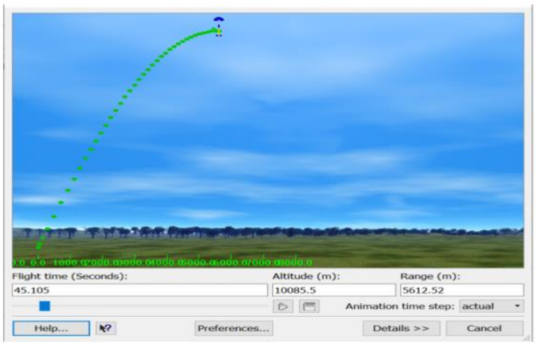

Figure 6: Rocket trajectory [4].

Figure 6 shows the rocket trajectory as it gets to apogee. As designed, the rocket would be recovered by both the main and drogue parachutes as specified in the input parameters. Also indicated is the time of flight which is 45.105 seconds, the maximum altitude attained which is 10,0085.5 m and range which is 5612.52 m.

The thrust versus time graph as indicated in Figure 7 to determine the maximum thrust generated by the propellent and the burn out time. As can be seen, the propellant generated about 20704 N and the propellant was exhausted after about 3 seconds.

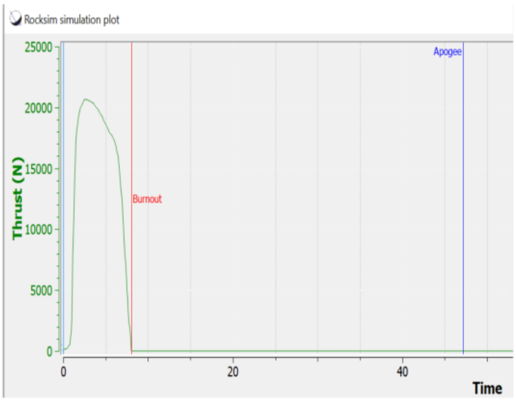

Figure 7: Thrust – time profile [4].

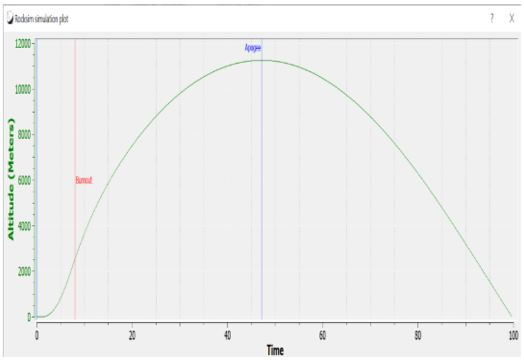

Figure 8: Altitude– time profile [4].

Figure 8 shows the maximum altitude the rocket attained and the time to achieve the height. The rocket gets to apogee at about 10,123.34 meters and at 44.0181 seconds.

As shown in Figure 9, the range that the rocket covered at altitude of 10,123.34 meters is 5611.7714 meters.

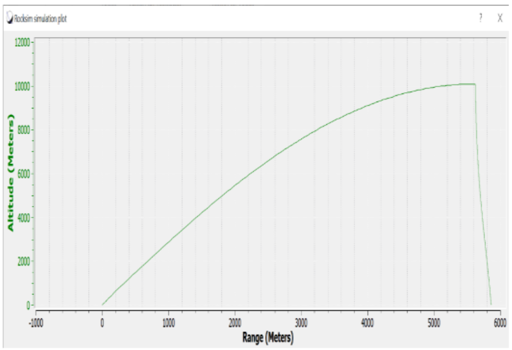

Figure 9: Altitude – range profile [4].

Figure 10 indicates the velocity rocket gained at every given time. The maximum velocity attained by the rocket is 632.1586 m/secs at 7.5251 seconds.

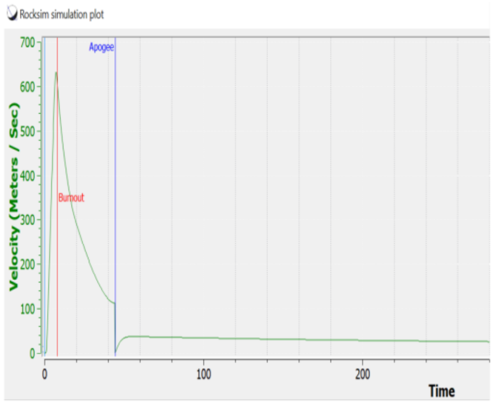

Figure 10: Velocity – time profile [4].

The acceleration versus time is shown in Figure 11. The maximum acceleration attained by the rocket is 135.37 m/s^2 at 3.3445 seconds.

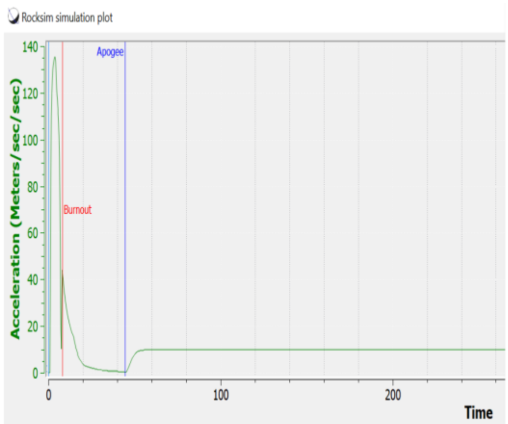

Figure 11: Acceleration – time profile [4].

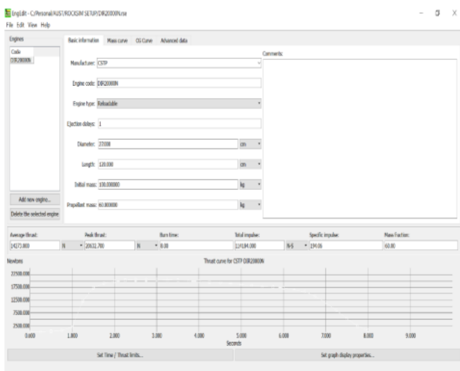

Figure 12: Basic propellant information [4].

Figure 12 shows the basic propellant information which includes the diameter, length, mass, average and peak thrust, burn time, total and specific impulses. The specific impulse achieved by the CSTP engine is 194.06 seconds [4].

4. CONCLUSION

The conclusion from this project are:

- It indicates the importance of material selection in designing the different components of a typical rocket.
- The material selected should be based on past experiences (heritage).
- Simple process in specifying the rocket components and ways to input them into the software.

5. REFERENCES

[1] Centre for Space Transport and Propulsion, Epe Lagos, Nigeria (2020). Sounding Rocket Design Handbook.

[2] www.nasa.gov.

[3] William Anderson (2004). Encyclopedia of Energy, Volume 5: Rocket Engines, Purdue University West Lafayette, Indiana, United States.

[4] Benneth Ifenna Okoli, Olusegun Samuel Sholiyi and Rasheed Olalekan Durojaye (2021). Design, analysis and simulation of a single stage rocket (launch vehicle) using RockSim. ResearchGate Publications, DOI: 10.13140/RG.2.2.10050.91848.

[5] Olusegun Samuel Sholiyi (2021). Lecture note on Launch vehicle and Launch pad designs and Advanced launch vehicle design. Department of Aerospace Engineering, African University of Science and Technology (AUST) Abuja, Nigeria - Institute of Space Science and Engineering (ISSE), Abuja, Nigeria.

International Journal of Science and Engineering Applications
Volume 10-Issue 04, 40 - 44, 2021, ISSN:- 2319 - 7560

Presenting the Multi-Objective Optimization Model of Search and Rescue Network

Md Mashum Billal
Department of Mechanical Engineering
University of Alberta
Edmonton, Canada

Maryam Maleki
Department of Systems Engineering
University of Arkansas at Little Rock
Little Rock, AR, USA

Abstract: The Search and Rescue Network (SAR) is a kind of emergency network that pursuit people in need or imminent danger. This paper aims using a priori optimization to demonstrate the optimal assignment of HFDF receivers to the Generalized Search and Rescue (GSAR) network, which is independent of the weighting of the transmitter areas. The mathematical model seeks two objectives, the first one is maximizing the expected number of LOBs for HFDF receivers. The second is providing a fair share number of HFDF receivers allowed to cover the frequency. The result shown the efficiency of presented model ran by CPLEX toolbox of MATLAB 2020 software.

Keywords: Search and Rescue Network; Priori Optimization; MATLAB 2020 Software; HFDF Receivers.

1. INTRODUCTION

Search and rescue network has different forms and each of them with unique risks and dangers to victim and responder [1], [2].The U.S. is founded and maintained a system of search and rescue (SAR) stations encompassing seas and oceans, these stations are responsible for receiving and processing signals from distressed ships, vessels and airplanes in order to initiate the emergency operations. The spark of any emergencies is the time when three or more stations receive and process the same distress signal since in order to find an approximation of distressed vessel three stations are required.

There are many optimization method for solving the search and rescue network. Among them, in this paper, we are planning to apply the multi-objective linear programming (MOLP) which is proposed by [5] to solve the problem as we will define in section 2. To solve their model, [5] convert the model to linear model in order to get the result in a fastetst time.

Simulation is other technique that some reasecrhers used in their studioes to find an answer near to the optimal result [6] [3]. Simulation optimization can be defined as finding the best input variable values of all options, and not evaluating each option explicitly. The objective of simulation optimisation is to minimize the resources spent in a simulation experiment while maximizing data. [6] used simulation technique to reduce the cost of production and the rate of energy waste during the transmission on electricity distribution systems. [3] applied a discrete event simulation approach and scenario discussion to encompass a set of operational decisions to manage the complexity of the system. Moreover, they employed the Arena simulation software for designing blood supply chain to provide a critical comparison of the two primary Key Performance Indicators shortage and outdated units of the BSC.

1.1 Relation Between Receiving Subsystems (RS) and Central Control (CC)

It is noted that each station in the SAR network has only one RS system, but the number of high frequency direction finding (HFDF) receivers in each station is different. In our problem, the number of HFDF receivers varies between 0 and 10. For more clarification, RS probes the entire frequency spectrum and has less sensitive and accurate than the HFDF. Moreover, RS has the limitation on small signal-to-noise ration unlike HFDF. Every HFDF receivers is allotted to a 1 MHz bund within the frequency spectrum.

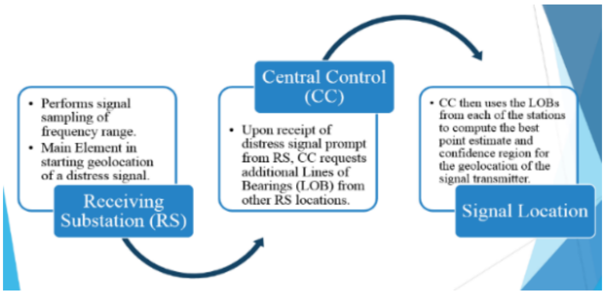

Figure. 1 Relationship between RS and CC

Prior to research background, the following schematic figure depicts the area of research in accordance with the receiving substation and estimated point of transmitted point and an acceptable circularized error radius.

1.2 Error Radius

The most recent research history on the topic of search and rescue culminated in optimal methods for the location of stations and frequency assignments. Since the subject is a well-acknowledged area of research, many previous researches had added to the body of knowledge. [4] thoroughly discussed the problem and different analytical approaches. He explained that "classical sensitivity analysis and tolerance analysis were used to analyze the frequency assignments generated by the different weight sequences. The weight sequence with all weights having equal value produced the most robust frequency assignments for all time blocks".

We followed the same footpath to recalculate the results once more time. Although [4] used ADBASE, LINGO and CPLEX IBM ILOG Studio also provided the same computer runs results, which are enclosed to this report as well.

As by [4] cited, the basis of his research is founded mainly on two antecedences, first, Steppe used a two-stage, network-flow multi-Objective linear integer programming (MOLIP) model [5] to determine the optimal position of the stations for the SAR problem. Second, Johnson's further work in this field has established optimal frequency assignments using the MOLIP network-flow model.

1.3 Research Objectives

The goal of this research is to use a priori optimization to show that the optimal assignment of HFDF receivers to the Generalized Search and Rescue (GSAR) network is independent of the weighting of the transmitter areas. This is achieved by examining the impact of changing the weight value of a specific transmitter area on the geolocation likelihood for that area. The mathematical model has two purposes, the first of which is to optimize the predicted number of LOBs for HFDF receivers. And the second is to have a reasonable share of the number of HFDF receivers allowed to cover the frequency [5].

2. MODEL FORMULATION

This section is an overview of the multi-objective linear programming (MOLP) and network programming formulas for the search and rescue network [6], [7], [2]. The weights for transmitter areas shall be given by the Department of Defense (DOD).

The notations, parameters, and variables are:

i: transmitter locations

j: receiving locations

k: frequency bands

F_{ik}: Probability of a distress signal from location i on frequency k

P_{ijk}: Probability that a distress signal from location i on frequency k is acquired by station j

W_{ij}: Probability that a line of bearing from station j is within the acceptable circularized error region defined for location i

U_i: The normalized weight (0 – 1 range) of a distress signal from location i

TN: The total number of HFDF receivers

FS: The fair share of HFDF receivers for each frequency

Where FS is the integer greater than or equal to the total number of HFDF receivers divided by the total number off frequencies to be covered.

X_{jk} = 1, if station j is assigned cover frequency k, otherwise 0

$Y_k = nY_k = \begin{cases} n \\ 0 \end{cases}$, if frequency k has excess coverage by n stations, otherwise 0

2.1 Objectives and Constraints

The model formulation for this multi-objective optimization model of a search and rescue network takes the following form [5]:

Objective Function 1: This objective function maximizes the estimated number of accurate bearing lines for HFDF receivers [2].

$$Max \sum_i \sum_j \sum_k U_i W_{ij} F_{ik} P_{ijk} X_{jk}$$

Objective Function 2: This objective function minimizes the excess coverage of HFDF receivers for each frequency.

$$Min \sum_k Y_k$$

Constraint 1: Limit the number of HFDF frequency assignments at each station to the number of receivers located at each station.

$$\sum_k X_{jk} \le m_j, \qquad \forall j$$

Constraint 2: This restriction allows at least two HFDF receivers to be allocated to cover each frequency.

$$\sum_j X_{jk} \ge 2, \qquad \forall k$$

Constraint 3: Determines the sum of excess coverage provided at each frequency. The vector Y_k is the indicator of excess coverage.

$$\sum_j X_{jk} - Y_k \le FS, \qquad \forall k$$

2.2 Obtained Data from DOD

A case study of actual data is provided, and the results are regenerated since the software changed. The following data is used to calculate the weights for the problem. Table 1 provides the probability of a signal being transmitted by a transmitter i on frequency k.

Table 1. Signal transmission and frequency probability

i / k	Frequency 1	Frequency 2	Frequency 3
Transmitter 1	0.04	0.04	0.04
Transmitter 2	0.00	0.00	0.01
Transmitter 3	0.03	0.05	0.05
Transmitter 4	0.00	0.00	0.00

Table 2 indicates the likelihood of a signal being transmitted from transmitter i to frequency k and acquired by station j.

Table 2. Probability of signal transmission and station acquisition

j	Transmitter				Transmitter				Transmitter			
	1	2	3	4	1	2	3	4	1	2	3	4
1	0.98	0.32	0.51	0.01	0.95	0.13	0.35	0.0	0.96	0.33	0.52	0.01
2	0.98	0.44	0.13	0.01	0.98	0.08	0.01	0.0	0.98	0.30	0.01	0.01
3	0.97	0.01	0.01	0.01	0.92	0.46	0.71	0.0	0.83	0.31	0.51	0.01
4	0.97	0.97	0.01	0.01	0.98	0.01	0.12	0.0	0.90	0.01	0.01	0.01
5	0.98	0.03	0.01	0.01	0.94	0.04	0.01	0.0	0.94	0.19	0.00	0.01

Table 3 indicates the likelihood that station j will receive a signal from the transmitter I when a signal has been transmitted.

Table 3. Probability of station receipt of signal

i / j	Station 1	Station 2	Station 3	Station 4	Station 5
Transmitter	0.3808	0.747	0.1951	0.121	0.7956
Transmitter	0.1477	0.1301	0.1140	0.0596	0.2504
Transmitter	0.1471	0.0892	0.1580	0.0834	0.1509
Transmitter	0.0515	0.7679	0.0615	0.0820	0.0427

Table 4 offers different weighting sequences for the nine solutions to the sample problem.

Table 4. Weighting sequence for the nine solutions to the sample problem

i /	Station	Station	Station	Station	Station	Station	Station	Station	Station
1	0.25	0.50	0.167	0.167	0.167	0.70	0.10	0.10	0.10
2	0.25	0.167	0.50	0.167	0.167	0.10	0.70	0.10	0.10
3	0.25	0.167	0.167	0.50	0.167	0.10	0.10	0.70	0.10
4	0.25	0.167	0.167	0.167	0.50	0.10	0.10	0.10	0.70

Table 5. Manual sensitivity analysis range for time block one weight

Weight #	Original Value	Low Value	High Value
20	0.203	1%	10%
22	0.145	16%	4%
27	0.203	6%	0%
30	0.145	28%	5%
31	0.203	11%	8%

Table 6. Manual sensitivity analysis range for time block six weights

Weight #	Original Value	Low Value	High Value
9	0.1491	10%	15%
20	0.1491	23%	4%
27	0.1491	3%	27%
30	0.1355	28%	4%
31	0.1897	11%	14%
40	0.1355	2%	13%

2.3 Methodology

The technique used was a constraint reduced feasible region method in a "toy problem" type of scenario where a condensed version of the larger problem was extracted and run to show that the calculations are accurate, and that the solution is viable.

The constraint reduced method to solve a MCLP is to "convert one of the two criterion functions, in this case $f_2(x)$, into a constraint, which is added to the existing constraint set $x \in X$." [6], [8], [9], [10]. The formulation of our toy problem therefore goes from the following objective function and constraint function notation:

$$\begin{aligned} max\ f_1(x) = {} & 0.0043*x11 + 0.004275*x12 + 0.004725*x13 \\ & + 0.007325*x21 + 0.00726*x22 + 0.00736*x23 \\ & + 0.001938*x31 + 0.0032*x32 + 0.002725*x33 \\ & + 0.001183*x41 + 0.0013*x42 + 0.001103*x43 \\ & + 0.007813*x51 + 0.007495*x52 \\ & + 0.0076*x53; \end{aligned}$$

$$min\ f_2(x) = -y1 - y2 - y3;$$

$$\begin{aligned} & x11 + x12 + x13 + x21 + x22 + x23 + x31 + x32 + x33 \\ & \quad + x41 + x42 + x43 + x51 + x52 \\ & \quad + x53 <= 15; \\ & X11 + x21 + x31 + x41 + x51 - e1 <= 3; \\ & x12 + x22 + x32 + x42 + x52 - e2 <= 3; \\ & X13 + x23 + X33 + X43 + x53 - e3 <= 3; \\ & X11 + x21 + x31 + x41 + x51 >= 2; \\ & X12 + X22 + X32 + X42 + X52 >= 2; \\ & X13 + x23 + x33 + x43 + x53 >= 2; \end{aligned}$$

To the following form:

$$\begin{aligned} max\ f_1(x) = {} & 0.0043*x11 + 0.004275*x12 + 0.004725*x13 \\ & + 0.007325*x21 + 0.00726*x22 + 0.00736*x23 \\ & + 0.001938*x31 + 0.0032*x32 + 0.002725*x33 \\ & + 0.001183*x41 + 0.0013*x42 + 0.001103*x43 \\ & + 0.007813*x51 + 0.007495*x52 + 0.0076*x53; \end{aligned}$$

$$-y1 - y2 - y3 = R;$$

$$\begin{aligned} & x11 + x12 + x13 + x21 + x22 + x23 + x31 + x32 + x33 \\ & \quad + x41 + x42 + x43 + x51 + x52 \\ & \quad + x53 <= 15; \end{aligned}$$

$$X11 + x21 + x31 + x41 + x51 - e1 <= 3;$$

$$x12 + x22 + x32 + x42 + x52 - e2 <= 3;$$

$$X13 + x23 + X33 + X43 + x53 - e3 <= 3;$$

$$X11 + x21 + x31 + x41 + x51 >= 2;$$

$$X12 + X22 + X32 + X42 + X52 >= 2;$$

$$X13 + x23 + x33 + x43 + x53 >= 2;$$

Where R is a "satisficing level for f_2". Then, "by graphically [and numerically] minimizing and maximizing f_2 over X, the feasible region defined by the original constraint set, we are able to find all the N-points.

The formulation of the linear program limits decision variables, X_{jk} and Y_k, to integer values. Specifically, X_{jk} must be equal to zero or one, while Y_k may take any positive integer value less than or equal to the number of receiving stations on the network.

For this toy problem, we utilized Lindo Systems' software, Lingo, to input and solve this linear problem. The values of R that we used ranged in value from 0 to -6. The detailed solution to this problem is presented in the solutions section and compared to the results from some of the other previous thesis papers.

3. SOLUTION OF CONSTRAINT REDUCED METHOD

As the solution procedure explained, we were able to run the model and obtain similar results mentioned in the references. In the appendices part, the Lingo program for the constraint reduced method for the toy problem and different values of R, ranging from 0 to -6, is provided. The *N*-Points acquired from this solution are tabulated in Table 7 and Table 8 below.

Table 7. *N*-points

R Values	X-space, N-points										
R	*X11*	*X12*	*X13*	*X21*	*X22*	*X23*	*X31*	*X32*	*X33*	*X41*	*X42*	*X43*
-6	1	1	1	1	1	1	1	1	1	1	1	1
-5	1	1	1	1	1	1	1	1	1	1	1	0
-4	1	1	1	1	1	1	1	1	1	0	1	0
-3	1	1	1	1	1	1	1	1	1	0	0	0
-2	1	1	1	1	1	1	0	1	1	0	0	0
-1	1	1	1	1	1	1	0	1	0	0	0	0
0	1	1	1	1	1	1	0	0	0	0	0	0

Table 8. *N*-points continued

X-space, N-points Continued									Y-space, N-Points	
X51	X52	X53	Y1	Y2	Y3	E1	E2	E3	$f_1(x)$	$f_2(x)$
1	1	1	0	0	0	2	2	2	0.069601	-6
1	1	1	0	0	0	2	2	1	0.068498	-5
1	1	1	0	0	0	1	2	1	0.067315	-4
1	1	1	0	0	0	1	1	1	0.066015	-3
1	1	1	0	0	0	0	1	1	0.064077	-2
1	1	1	0	0	0	0	1	0	0.061352	-1
1	1	1	0	0	0	0	0	0	0.058152	0

The following solution is gained through the thesis's results, and it is presented that the Lingo's output is closely matched the EVAL computer software developed by DOD.

```
        X space N-points                 Y space N-points
r2      (x11, ..., x53, e1, e2, e3)      (f1(X), f2(X))
--------------------------------------------------------------
-6  (1,1,1,1,1,1,1,1,1,1,1,1,1,1,1,2,2,2)  (0.069602, -6) A
-5  (1,1,1,1,1,1,1,1,1,1,1,0,1,1,1,2,2,1)  (0.068499, -5) B
-4  (1,1,1,1,1,1,1,1,1,0,1,0,1,1,1,1,2,1)  (0.067316, -4) C
-3  (1,1,1,1,1,1,1,1,1,0,0,0,1,1,1,1,1,1)  (0.066016, -3) D
-2  (1,1,1,1,1,1,0,1,1,0,0,0,1,1,1,0,1,1)  (0.064078, -2) E
-1  (1,1,1,1,1,1,0,1,0,0,0,0,1,1,1,0,1,0)  (0.061353, -1) F
 0  (1,1,1,1,1,1,0,0,0,0,0,0,1,1,1,0,0,0)  (0.058153,  0) G
```

Figure. 2 Solution

The following graphical representation depicts the Y-space which is the optimal values given from the trade-offs between two objective functions.

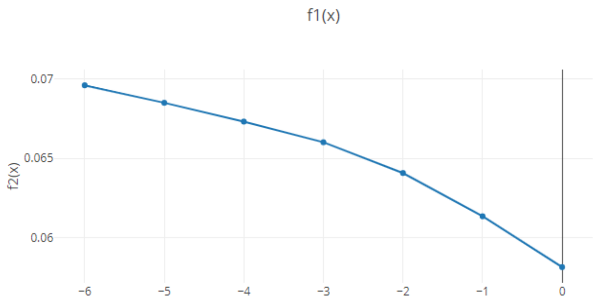

Figure. 2 Graph of *N*-points in *Y*-space demonstrating the efficient frontier

4. CONCLUSION

This paper used a priori optimization to demonstrate the optimal assignment of HFDF receivers to the Generalized Search and Rescue (GSAR) network, which is independent of the weighting of the transmitter areas. The model objective presented was to optimize the estimated number of LOBs for HFDF receivers and to provide a reasonable share of the number of HFDF receivers allowed to cover the frequency. Although optimization models are of remarkable importance when it boils down to accuracy, being time consuming and engaging computational resources are the reasons to consider artificial intelligence approaches too, such as Simulated Annealing algorithm [11], Genetic Algorithm [12], [13], [14], discrete event simulation [6] [3], and heuristic algorithms [15]–[17].

5. REFERENCE

[1] R. R. Murphy *et al.*, "Search and Rescue Robotics," in *Springer Handbook of Robotics*, Berlin, Heidelberg: Springer Berlin Heidelberg, 2008, pp. 1151–1173.

[2] N. Razi and M. Karatas, "A multi-objective model for locating search and rescue boats," *Eur. J. Oper. Res.*, vol. 254, no. 1, pp. 279–293, Oct. 2016, doi: 10.1016/j.ejor.2016.03.026.

[3] M. Arani, X. Liu, and S. Abdolmaleki, "Scenario-Based Simulation Approach for An Integrated Inventory Blood Supply Chain System," in *2020 Winter Simulation Conference (WSC)*, Dec. 2020, pp. 1348–1359, doi: 10.1109/WSC48552.2020.9384018.

[4] J. C. I. Jr, "An A Priori Multiobjective Optimization Model of a Search and Rescue Network," 1992.

[5] S. Hayat, E. Yanmaz, T. X. Brown, and C. Bettstetter, "Multi-objective UAV path planning for search and rescue," in *2017 IEEE International Conference on Robotics and Automation (ICRA)*, May 2017, pp. 5569–5574, doi: 10.1109/ICRA.2017.7989656.

[6] M. Arani, M. Dastmard, Z. D. Ebrahimi, M. Momenitabar, and X. Liu, "Optimizing the Total Production and Maintenance Cost of an Integrated Multi-Product Process and Maintenance Planning (IPPMP) Model," in *2020 IEEE International*

Symposium on Systems Engineering (ISSE), Oct. 2020, pp. 1–8, doi: 10.1109/ISSE49799.2020.9272236.

[7] M. MomeniTabar, Z. D. Ebrahimi, S. H. Hosseini, and M. Arani, "A Proposed Lean Distribution System for Solar Power Plants Using Mathematical Modeling and Simulation Technique," 2020, doi: 978-1-7281-9677-0/20/$31.00.

[8] A. Mehrez, M. Eben-Chaime, and J. Brimberg, "Locational Analyses of Military Intelligence Ground Facilities : EMOR," MORS, 1996, pp. 61–69.

[9] S. Hayat, E. Yanmaz, C. Bettstetter, and T. X. Brown, "Multi-objective drone path planning for search and rescue with quality-of-service requirements," *Auton. Robots*, vol. 44, no. 7, pp. 1183–1198, Sep. 2020, doi: 10.1007/s10514-020-09926-9.

[10] I. Nielsen, G. Bocewicz, and S. Saha, "Multi-agent Path Planning Problem Under a Multi-objective Optimization Framework," pp. 5–14, 2021, doi: 10.1007/978-3-030-53829-3_1.

[11] M. Arani, M. Momenitabar, Z. Dehdari Ebrahimi, and X. Liu, "Unrelated Parallel Machine Scheduling Problem Considering Inventories Subject to Resource Constraints and Due Dates," 2021.

[12] M. M. Billal and M. M. Hossain, "Multi-Objective Optimization for Multi-Product Multi-Period Four Echelon Supply Chain Problems Under Uncertainty," *J. Optim. Ind. Eng.*, vol. 13, no. 1, pp. 1–17, 2020, doi: 10.22094/joie.2018.555578.1529.

[13] A. S. Abir, I. A. Bhuiyan, M. Arani, and M. M. Billal, "Multi-Objective Optimization for Sustainable Closed-Loop Supply Chain Network Under Demand Uncertainty: A Genetic Algorithm," 2020.

[14] B. Afshar-Nadjafi and M. Arani, "Multimode Preemptive Resource Investment Problem Subject to Due Dates for Activities: Formulation and Solution Procedure," *Adv. Oper. Res.*, vol. 2014, pp. 1–10, 2014, doi: 10.1155/2014/740670.

[15] Y. Chan, J. A. Fowe, and M. Arani, "Routing in a Stochastic Network with Nonrecurrent Incidents: Behavioral Interpretation of Dynamic Traffic Assignment," *ASCE-ASME J. Risk Uncertain. Eng. Syst. Part A Civ. Eng.*, vol. 6, no. 1, p. 4020002, Mar. 2020, doi: 10.1061/AJRUA6.0001033.

[16] M. Arani, M. M. Rezvani, H. Davarikia, and Y. Chan, "Routing of Electric Vehicles in a Stochastic Network with Non-recurrent Incidents," *Am. Sci. Res. J. Eng. Technol. Sci.*, Dec. 2019.

[17] M. Maleki, Y. Chan, and M. Arani, "Impact of Autonomous Vehicle Technology on Long Distance Travel Behavior," *IISE Annu. Conf. Expo 2020*, Jan. 2021.